Preprints of the 18th IFAC World Congress
Milano (Italy) August 28 - September 2, 2011

An SDRE-Based Approach for HIV Feedback Control and Control of Thin Film Growth in a CVD Reactor ⋆

H. T. Banks * **S. C. Beeler** ** **Hee-Dae Kwon** ***
B. M. Lewis **** **J. A. Toivanen** † **H. T. Tran** *

* *Department of Mathematics, Box 8205, North Carolina State University, Raleigh, NC 27695 USA (e-mails: htbanks@ncsu.edu (Banks), tran@ncsu.edu (Tran))*
** *Lockheed Martin Missiles & Space, 1111 Lockheed Martin Way, Sunnyvale, CA 94089 USA (e-mail: scott.c.beeler@lmco.com)*
*** *Department of Mathematics, Inha University, Incheon, South Korea (e-mail: hdkwon@inha.ac.kr)*
**** *MIT Lincoln Laboratory, 244 Wood Street, Lexington, MA 02420 USA (e-mail: blewis@ll.mit.edu)*
† *Institute for Computational and Mathematical Engineering, Durand Building 500, Room 023A Stanford University, Stanford, CA 94305 USA (e-mail: toivanen@stanford.edu)*

Abstract: A number of computational methodologies have been proposed in the literature to design and synthesize feedback controls when the plant is modeled by nonlinear dynamical systems. One of the highly promising and rapidly emerging methodologies for designing nonlinear controllers is the state-dependent Riccati equation (SDRE) method in the context of the nonlinear regulator problem. In essence, SDRE mimics the linear quadratic regulator theory by using direct parametrization to rewrite the nonlinear state function as a product of a state-dependent coefficient matrix with the state vector. This paper presents an overview of our successful effort on the application of SDRE for the regulation of the growth of thin films in a high pressure chemical vapor deposition (CVD) and for the development of optimal dynamic multi-drug therapies for human immunodeficiency virus (HIV) infection.

Keywords: HIV, CVD, nonlinear feedback control, tracking control, nonlinear compensator, state-dependent Riccati equation.

1. INTRODUCTION

Linear quadratic regulation (LQR) is a well established and effective theory for the synthesis of control laws for linear systems. However, most mathematical models for biological systems, including HIV dynamics with immune response Adams et al. (2005), as well as those for physical processes, such as those arising in the microelectronic industry Banks et al. (2002), are inherently nonlinear. A number of methodologies exist for the control design and synthesis of these complex nonlinear systems. One of the highly promising methodologies for designing nonlinear controllers is the state-dependent Riccati equation (SDRE) approach in the context of the nonlinear regulator problem (see for example, Cloutier et al. (1996); Banks et al. (2007)). In essence, the SDRE method is a systematic way of designing nonlinear feedback controllers by factoring the state dependent nonlinearity of the state equations as a product of a state dependent matrix with the state vector. That is, by using direct parameterization the nonlinear system is brought to a linear structure with state dependent coefficient matrices. This parametrization is however not unique and thus some flexibility in design is permissible. The state feedback control law is then given in terms of the solution of a state dependent Riccati equation. As shown in Banks et al. (2002), the SDRE method is a powerful approach that is readily applicable to the nonlinear tracking and nonlinear state estimation problems, since it is closely related to the algebraic Riccati equation-based method used to find the feedback controls in the linear cases.

In this paper, we report on the successful use of SDRE in a biological and an engineering application. In particular, we present the application of SDRE for combined drug/immune response control of HIV infection. On another application, we used SDRE in the development of nonlinear feedback control methods for real-time implementation on a chemical vapor deposition reactor. The problems are optimal tracking problems (for regulation of the growth of thin films in a high-pressure chemical vapor deposition (HPCVD) reactor) that employ state-dependent Riccati gains with nonlinear observations and

⋆ This research was supported in part by Grant Number R01AI071915-07 from the National Institute of Allergy and Infectious Diseases and in part by the Air Force Office of Scientific Research under grant number FA9550-09-1-0226.

the resulting dual state-dependent Riccati equations for the compensator gains.

2. SDRE-BASED FEEDBACK CONTROLLERS

In this section we formulate the optimal control problem where it is assumed that all state variables are available for feedback. In particular, the cost functional is given by the integral

$$J(x_0,u)=\frac{1}{2}\int_{t_0}^{\infty}(x^TQx+u^TRu)\,dt, \tag{1}$$

where $x\in\Re^n$, $u\in\Re^m$, $Q\in\Re^{n\times n}$ is symmetric positive semidefinite (SPSD), and $R\in\Re^{m\times m}$ is symmetric positive definite (SPD). Associated with the performance index (1) are the nonlinear dynamics

$$\dot{x}=f(x)+B(x)u, \tag{2}$$

where $f(x)$ is a nonlinear function in C^k and $B(x)\in\Re^{n\times m}$ is a matrix-valued function. Rewriting the nonlinear dynamics (2) in the state-dependent coefficient (SDC) form $f(x)=A(x)x$, we have

$$\dot{x}=A(x)x+B(x)u, \tag{3}$$

where, in general, $A(x)$ is unique only if x is scalar Cloutier et al. (1996).

The Hamiltonian for the optimal control problem (1)-(3) is given by

$$H(x,u,\lambda)=\frac{1}{2}(x^TQx+u^TRu)+\lambda^T(A(x)x+B(x)u). \tag{4}$$

From the Hamiltonian, the necessary conditions for the optimal control are found to be

$$\dot{\lambda}=-Qx-\left[\frac{\partial\,(A(x)x)}{\partial x}\right]^T\lambda-\left[\frac{\partial\,(B(x)u)}{\partial x}\right]^T\lambda, \tag{5}$$

$$\dot{x}=A(x)x+B(x)u, \tag{6}$$

and

$$0=Ru+B^T(x)\lambda. \tag{7}$$

Let $A_{i:}$ denote the ith row of $A(x)$ and $B_{i:}$ denote the ith row of $B(x)$. Then

$$\begin{aligned}\frac{\partial\,(A(x)x)}{\partial x}&=A(x)+\frac{\partial\,(A(x))}{\partial x}x\\&=A(x)+\begin{bmatrix}\frac{\partial A_{1:}}{\partial x_1}x&\dots&\frac{\partial A_{1:}}{\partial x_n}x\\\vdots&\ddots&\vdots\\\frac{\partial A_{n:}}{\partial x_1}x&\dots&\frac{\partial A_{n:}}{\partial x_n}x\end{bmatrix}\end{aligned} \tag{8}$$

and

$$\frac{\partial\,(B(x)u)}{\partial x}=\begin{bmatrix}\frac{\partial B_{1:}}{\partial x_1}u&\dots&\frac{\partial B_{1:}}{\partial x_n}u\\\vdots&\ddots&\vdots\\\frac{\partial B_{n:}}{\partial x_1}u&\dots&\frac{\partial B_{n:}}{\partial x_n}u\end{bmatrix}. \tag{9}$$

Mimicking the LQR theory, the co-state is assumed to be of the form $\lambda=\Pi(x)x$ (note the state dependency). Using this form for λ in equation (7) we obtain a feedback control $u=-R^{-1}B^T(x)\Pi(x)x$. Substituting this control back into (6), we find $\dot{x}=A(x)x-B(x)R^{-1}B^T(x)\Pi(x)x$. To find the matrix-valued function $\Pi(x)$, we differentiate $\lambda=\Pi(x)x$ with respect to time along a trajectory to obtain

$$\begin{aligned}\dot{\lambda}&=\dot{\Pi}(x)x+\Pi(x)\dot{x}\\&=\dot{\Pi}(x)x+\Pi(x)A(x)x-\Pi(x)B(x)R^{-1}B^T(x)\Pi(x)x,\end{aligned}$$

where we use the notation

$$\dot{\Pi}(x)=\sum_{i=1}^{n}\Pi_{x_i}(x)\dot{x}_i(t).$$

If we set this equal to $\dot{\lambda}$ from (5), we find

$$\begin{aligned}&\dot{\Pi}(x)x+\Pi(x)A(x)x-\Pi(x)B(x)R^{-1}B^T(x)\Pi(x)x\\&\quad=-Qx-\left[A(x)+\frac{\partial\,(A(x))}{\partial x}x\right]^T\Pi(x)x\\&\qquad-\left[\frac{\partial\,(B(x)u)}{\partial x}\right]^T\Pi(x)x.\end{aligned}$$

Rearranging terms we find

$$\begin{aligned}\Bigg[\Bigg(\dot{\Pi}(x)+&\left[\frac{\partial\,(A(x))}{\partial x}\right]^T\Pi(x)+\left[\frac{\partial\,(B(x)u)}{\partial x}\right]^T\Pi(x)\Bigg)\\&+\big(\Pi(x)A(x)+A^T(x)\Pi(x)\\&-\Pi(x)B(x)R^{-1}B^T(x)\Pi(x)+Q\big)\Bigg]x=0.\end{aligned}$$

If we assume that $\Pi(x)$ solves the SDRE, which is given by

$$\begin{aligned}&\Pi(x)A(x)+A^T(x)\Pi(x)\\&\qquad-\Pi(x)B(x)R^{-1}B^T(x)\Pi(x)+Q=0,\end{aligned} \tag{10}$$

then the following condition must be satisfied for optimality:

$$\dot{\Pi}(x)+\left[\frac{\partial\,(A(x))}{\partial x}\right]^T\Pi(x)+\left[\frac{\partial\,(B(x)u)}{\partial x}\right]^T\Pi(x)=0. \tag{11}$$

To be consistent with Cloutier et al. (1996), we will refer to (11) as the *Optimality Criterion*. The suboptimal control for (1) and (3) is found by solving (10) for $\Pi(x)$. Then, the optimal control problem has the suboptimal solution

$$u=-K(x)x \text{ where } K(x)=R^{-1}B^T(x)\Pi(x). \tag{12}$$

If we denote the ϵ-ball around z as

$$\mathcal{B}_\epsilon(z)=\{x:\|x-z\|<\epsilon\},$$

the following theorem establishes that the controlled system (3) with the nonlinear feedback controller (12) is asymptotically stable Banks et al. (2007).

Theorem 1. Assuming that the system

$$\dot{x}=f(x)+B(x)u$$

is such that $f(x)$ and $\frac{\partial f(x)}{\partial x_j}(j=1,\dots,n)$ are continuous in x for all $\|x\|\le\hat{r}$, $\hat{r}>0$, and that $f(x)$ can be written as $f(x)=A(x)x$ (in SDC form). Assume further that $A(x)$ and $B(x)$ are continuous and the system defined by (1) and (3) is a detectable and stabilizable parameterization in some nonempty neighborhood of the origin $\Omega\subseteq\mathcal{B}_{\hat{r}}(0)$. Then the system with the control given by (12) is locally asymptotically stable.

3. NUMERICAL METHODS FOR SOLVING SDRE

In general, one cannot find an exact solution to the SDRE analytically. Currently, one approach for solving the SDRE is via symbolic software packages such as `Maple` or `Mathematica`. However, once the dynamics of the system become complicated it is difficult to obtain a solution in this manner and it becomes necessary to approximate the solution. The approximated methods that we employed

included the Taylor series method and the interpolation method. The Taylor series method works for systems with constant control coefficients (B is not dependent on x). This uses the methodology of Taylor series approximations and is only effective locally. The interpolation method can be used for more complex systems. This method involves varying the state over the domain of interest, solving for and storing the control $u(x)$, the SDRE solution $\Pi(x)$, or the SDRE gain $K(x)$ in a grid and interpolating over the stored solutions to approximate the control. For more detailed discussions of these methodologies we refer the reader to the article Banks et al. (2007).

4. APPLICATIONS OF SDRE

In this section, we present two applications where we have successfully applied the SDRE method for the design and synthesis of nonlinear feedback controllers.

4.1 Dynamic Multidrug Therapies for HIV

Anti-HIV drugs fall into three major categories: nucleoside reverse transcriptase inhibitors (NRTIs), non-nucleoside reverse transcriptase inhibitors (NNRTIs), and protease inhibitors (PIs). The first two drug categories act by preventing HIV RNA from being converted into DNA, effectively blocking integration of the viral code into the host cell genome. On the other hand, the third category affects the viral assembly process in the final stage of the viral life cycle, preventing the proper cutting and structuring of the viral proteins before their release from the host cell.

The dynamics of HIV infection are described by the following nonlinear system of differential equations:

$$\begin{aligned}
\dot{T}_1 &= \lambda_1 - d_1 T_1 - (1-\epsilon_1) k_1 V_I T_1 \\
\dot{T}_2 &= \lambda_2 - d_2 T_2 - (1-f\epsilon_1) k_2 V_I T_2 \\
\dot{T}_1^* &= (1-\epsilon_1) k_1 V_I T_1 - \delta T_1^* - m_1 E T_1^* \\
\dot{T}_2^* &= (1-f\epsilon_1) k_2 V_I T_2 - \delta T_2^* - m_2 E T_2^* \\
\dot{V}_I &= (1-\epsilon_2) N_T \delta (T_1^* + T_2^*) \\
&\quad - \left[c + (1-\epsilon_1)\rho_1 k_1 T_1 + (1-f\epsilon_1)\rho_2 k_2 T_2\right] V_I \\
\dot{V}_{NI} &= \epsilon_2 N_T \delta (T_1^* + T_2^*) - c V_{NI} \\
\dot{E} &= \lambda_E + b_E \frac{T_1^* + T_2^*}{T_1^* + T_2^* + K_b} E \\
&\quad - d_E \frac{T_1^* + T_2^*}{T_1^* + T_2^* + K_d} E - \delta_E E.
\end{aligned} \tag{13}$$

In the model (13), the state variables are: T_1, the uninfected CD4+ T-cells; T_2, the uninfected target cells of second kind; T_1^*, the infected T-cells; T_2^*, the infected target cells of second kind; V_I, the infectious virus; V_{NI}, the non infectious virus; and E, the immune effectors. The controllers ϵ_1 and ϵ_2 represent RTI and PI "efficacies", respectively. We do not give precise biological definitions for the target cells of second kind and the immune effectors. They could, for example, be related to macrophages and cytotoxic T-lymphocytes, respectively. For a more detailed description of the variables, rationale and parameter values for the model (13) we refer the reader to the article Adams et al. (2005). This model exhibits several steady states. These are described and analyzed in Adams et al. (2005) with the non infectious virus V_{NI} state always being zero in these steady states. We are particularly interested in the so-called "healthy" steady state (low viral load, high immune effector level, and reasonably large target cell T_1 counts) given by

$$\begin{aligned}
T_1 &= 967.839 \frac{\text{cells}}{\text{mm}^3}, & T_2 &= 0.621 \frac{\text{cells}}{\text{mm}^3}, \\
T_1^* &= 0.076 \frac{\text{cells}}{\text{mm}^3}, & T_2^* &= 0.006 \frac{\text{cells}}{\text{mm}^3}, \\
V_I &= 0.415 \frac{\text{virions}}{\text{mm}^3}, & V_{NI} &= 0.0 \frac{\text{virions}}{\text{mm}^3}, \\
E &= 353.108 \frac{\text{cells}}{\text{mm}^3},
\end{aligned} \tag{14}$$

which was also shown to be locally asymptotically stable. This means that after a sufficiently small perturbation from (14), the trajectory of the state returns to the stable equilibrium (14).

We formulate the problem of finding an effective multidrug therapy as a tracking problem. To this end, we define the objective functional

$$\begin{aligned}
J(x,u) = &\frac{1}{2}\int_0^\infty \{(V_I - 0.415)^2 + 10(E - 353.108)^2 \\
&+ (\epsilon_1/\epsilon_1^{\max})^2 + (\epsilon_2/\epsilon_2^{\max})^2\} dt,
\end{aligned} \tag{15}$$

where V_I is the number of free virus and E represents the immune response. The control variable ϵ_1, where $0 \le \epsilon_1 \le \epsilon_1^{\max}$, denotes the "efficacy" of the reverse transcriptase inhibitor. Similarly, the control variable ϵ_2, $0 \le \epsilon_2 \le \epsilon_2^{\max}$, represents the "efficacy" of the protease inhibitor. We note that throughout we use the somewhat nonstandard terminology "efficacy" interchangeably with the control level for the two drugs. The weights in (15) have been determined a priori through a series of numerical experiments.

Using the following notation

$$u = \begin{pmatrix} \epsilon_1 \\ \epsilon_2 \end{pmatrix}, \quad \check{u} = \begin{pmatrix} 0 \\ 0 \end{pmatrix}, \quad \text{and} \quad \hat{u} = \begin{pmatrix} \epsilon_1^{\max} \\ \epsilon_2^{\max} \end{pmatrix},$$

the optimal tracking control problem is to find a dynamic multidrug therapy $u(t)$ satisfying

$$\min_{\check{u} \le u(t) \le \hat{u}} J(x(t), u(t)), \tag{16}$$

where $x(t) = (T_1, T_2, T_1^*, T_2^*, V_I, V_{NI}, E)^T$ is the state variable satisfying the state equation given by (13) with initial condition $x(0) = x_0$.

We note that our mathematical model for HIV dynamics (13) is nonlinear. Hence, for the design of feedback controllers to find a suboptimal treatment strategy we employ the SDRE method as described in Section 2. In particular, for the HIV model our parametrization choice for the nonlinear system involves the exact local linearization of the nonlinear state-dependent system dynamics at the current state of the system. In the following we will present simulation results where we assumed that full state observations are available for feedback for the derivation of the suboptimal nonlinear feedback controllers). In particular, we consider a physiological condition in which a patient who has not taken medication after HIV infection and the disease progression is proceeding towards the unhealthy steady state (high virus load and low immune response). The initial conditions for this case study are given by:

$$\begin{aligned} T_1 &= 163.573\frac{\text{cells}}{\text{mm}^3}, & T_2 &= 0.005\frac{\text{cells}}{\text{mm}^3}, \\ T_1^* &= 11.945\frac{\text{cells}}{\text{mm}^3}, & T_2^* &= 0.046\frac{\text{cells}}{\text{mm}^3}, \\ V_I &= 63.919\frac{\text{virions}}{\text{mm}^3}, & V_{NI} &= 0.0\frac{\text{virions}}{\text{mm}^3}, \\ E &= 0.024\frac{\text{cells}}{\text{mm}^3}. \end{aligned} \tag{17}$$

In this example we also assume that the maximum "efficacies" to be $\epsilon_1^{\max} = 0.75$ and $\epsilon_2^{\max} = 0.3$. Finally, the medication will be administered only when the condition

$$V_I + V_{NI} > 1.0\frac{\text{virions}}{\text{mm}^3} \tag{18}$$

is satisfied. Our control problem is to find a suboptimal nonlinear feedback controller that can transfer the system from the unhealthy state (17) to the "healthy" equilibrium state (14) in finite time. For a detailed discussion on how to implement the SDRE method for this application we refer the reader to Banks et al. (2006). Figure 1 presents

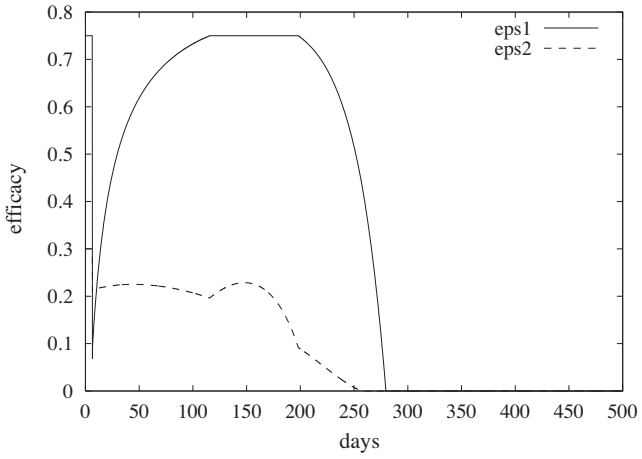

Fig. 1. The medication efficacy levels starting from the unhealthy steady state

the resulting treatment regimen and Figure 2 depicts the corresponding progressions of the state variables. At about 300 days the state variables have reached near equilibrium and start to oscillate in the neighborhood of the stable "healthy" steady state (14). The oscillations are not numerical artifacts but are likely consequences of the interaction (product) terms that appear in the mathematical model (13). It is noted that when the system reaches the stable equilibrium state, medication is no longer required.

4.2 Control of Thin Film Growth in an HPCVD Reactor

Chemical vapor deposition (CVD) is an important industrial technique used to grow thin films with certain desired properties. This process involves the deposition of precursor vapor sources onto a heated substrate where they react to form the desired material. Extending the CVD procedure to higher pressures increases our ability to control the thermal decomposition of certain source gases, and expands the range of compositions which can be produced at optimal process temperatures. Higher pressures can also result in faster film deposition and throughput,

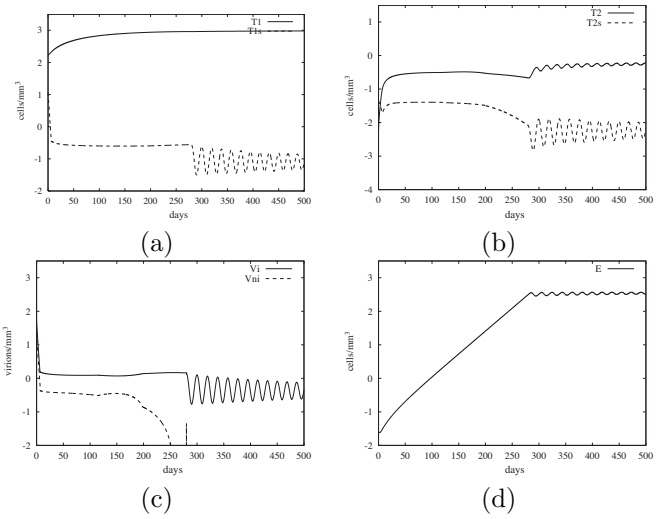

Fig. 2. Plots of the state variables using the stopping criterion based on the viral load with the y-axis in $\log_{10}$-scale. (a) Plots of T_1 and T_1^*. (b) Plots of T_2 and T_2^*. (c) Plots of V_I and V_{NI}. (d) Plot of E

an advantage in time-intensive applications in the semiconductor industry. The challenge in high-pressure chemical vapor deposition (HPCVD) is that it is significantly more difficult to control than the low-pressure process, as the higher pressure introduces source vapor gas flow dynamics in the place of low-pressure ballistic source vapor pulses.

The gas-phase flow model for the HPCVD reactor represents the flow of precursor species from the reactor inlet to the substrate surface, with the transport process dynamics given by the partial differential equations for continuity, momentum, energy and species balances, including multiple species and gas-phase reactions. These equations are considered for a case with only trace amounts of the precursors mixed with the carrier gas (N_2) in the reactor operating at a pressure of 10 atmospheres. With this dilute assumption a quasi-steady model can be constructed, with the continuity, momentum and energy equations solved as steady-state equations, based on the properties of the dominant carrier gas and independent of the reactant concentrations:

$$\overrightarrow{\nabla} \cdot (\rho \overrightarrow{v}) = 0 \tag{19}$$

$$\rho \overrightarrow{v} \cdot \overrightarrow{\nabla} \overrightarrow{v} = -\overrightarrow{\nabla} P + \overrightarrow{\nabla} \cdot \overrightarrow{\tau} - \rho \overrightarrow{g} \tag{20}$$

$$\rho c_p \overrightarrow{v} \cdot \overrightarrow{\nabla} T = \overrightarrow{\nabla} \cdot (k \overrightarrow{\nabla} T), \tag{21}$$

where the viscous stress tensor is given by

$$\overrightarrow{\tau} = -\frac{2}{3}\mu(\overrightarrow{\nabla} \cdot \overrightarrow{v})\overrightarrow{I} + \mu(\overrightarrow{\nabla} \overrightarrow{v} + \overrightarrow{\nabla} \overrightarrow{v}^T). \tag{22}$$

Here $\overrightarrow{v}$, T and P are the velocity, temperature and pressure, respectively, $\overrightarrow{g}$ is the gravitational acceleration, and μ, c_p and k are the viscosity, specific heat and conductivity of the carrier gas. The density variation is modeled as

$$\rho = \rho_0[1 - \beta(T - T_0)], \tag{23}$$

with a reference temperature T_0, a reference density ρ_0 calculated from the ideal gas law at the reference temperature and reactor pressure, and the volume coefficient of expansion $\beta = 1/T$.

Our numerical model is a three-dimensional rectangular-box-shaped domain where a side-view cross-section of this model is shown in Fig. 3, with the very small height not to scale (see Banks et al. (2002) for discussions on the boundary conditions and physical parameters). The

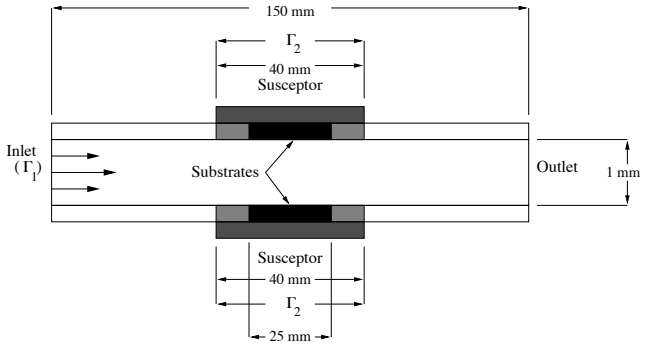

Fig. 3. HPCVD reactor side-view cross-section (not to scale). The width of the reactor is 50 mm.

solutions for velocity and temperature that are found from equations (19)-(23) can then be used in the solution of the time-dependent species equations for the precursor mass fractions,

$$\begin{aligned}
\frac{\partial Y_n}{\partial t} + \overrightarrow{v}\cdot\overrightarrow{\nabla} Y_n &= \frac{1}{\rho}\overrightarrow{\nabla}\cdot(\rho D_n \overrightarrow{\nabla} Y_n) + \sum_{i=1}^{N_R} r_{ni} \\
Y_n(0,\overrightarrow{x}) &= 0, \\
\frac{\partial Y_1(t,\overrightarrow{x})}{\partial \overrightarrow{n}} &= \frac{1}{\epsilon}\left(Y_1(t,\overrightarrow{x}) - u_1\right), \text{ at inflow}\Gamma_1 \\
\frac{\partial Y_n(t,\overrightarrow{x})}{\partial \overrightarrow{n}} &= \frac{1}{\epsilon} Y_n(t,\overrightarrow{x}), \text{ at inflow } \Gamma_1 \text{ (n=2,3)} \\
\frac{\partial Y_n(t,\overrightarrow{x})}{\partial \overrightarrow{n}} &= \frac{1}{\epsilon} Y_n(t,\overrightarrow{x}), \text{ at substrates } \Gamma_2 \\
\frac{\partial Y_n(t,\overrightarrow{x})}{\partial \overrightarrow{n}} &= 0, \text{ at walls, outflow,}
\end{aligned} \tag{24}$$

We note that the time-dependent species equations are formulated with penalty Neumann boundary conditions to prepare the system for the Galerkin procedure and for the tracking control problem to be discussed later. The parameter ϵ is a small parameter (for our simulations we use $\epsilon = 10^{-3}$). With sufficient regularity assumed, it can be argued that as $\epsilon \to 0$ the solution to (24) approximates the solution to the species transport problem with appropriate and physical Dirichlet boundary conditions (see Barrett and Elliot (1986) for related discussions).

In the HPCVD computational control experiments to follow we consider trimethylgallium, or TMG ($Ga(CH_3)_3$), and phosphine (PH_3) as source materials for the growth of the III-V film gallium phosphide (GaP). For the gallium transport we will consider three gas-phase species (aside from the carrier gas): Y_1 representing the mass fraction of TMG, Y_2 that of dimethylgallium (DMG), and Y_3 that of monomethylgallium (MMG).

We will assume that there are $N_R = 2$ significant gas phase reaction mechanisms for the gallium species. There is the reaction for the decomposition of TMG to DMG and a methyl molecule, $Ga(CH_3)_3 \to Ga(CH_3)_2 + CH_3$ (reaction 1), and the decomposition of DMG to MMG and a methyl molecule, $Ga(CH_3)_2 \to GaCH_3 + CH_3$ (reaction 2). These decompositions can be described as first-order Arrhenius reactions with rates of production given by

$$r_{ni} = \nu_{ni}\frac{W_n}{W_{m_i}} k_i e^{-E_i/RT} Y_{m_i}, \tag{25}$$

where m_i is the number of the species which is the source in reaction i. The parameter ν_{ni} is the stoichiometric constant for species n in reaction i, W_n and W_{m_i} are the molecular weights of those particular species, and k_i is the rate constant and E_i the activation energy for reaction i (see Banks et al. (2002) for the values of these physical parameters).

The above gas-phase model will be linked to a modified version of the reduced order surface kinetics (ROSK) model developed in Beeler et al. (1999). From the species mass fractions Y_n, the flux of gallium to a specific point $\overrightarrow{x}_p$ at the center of one of the substrate surfaces is given by

$$\begin{aligned}
q(\overrightarrow{Y}) = -\rho \Bigg[& D_1 \frac{W_{Ga}}{W_1}\frac{\partial Y_1}{\partial \overrightarrow{n}}\bigg|_{\overrightarrow{x}_p} \\
& + D_2 \frac{W_{Ga}}{W_2}\frac{\partial Y_2}{\partial \overrightarrow{n}}\bigg|_{\overrightarrow{x}_p} + D_3 \frac{W_{Ga}}{W_3}\frac{\partial Y_3}{\partial \overrightarrow{n}}\bigg|_{\overrightarrow{x}_p} \Bigg].
\end{aligned} \tag{26}$$

The molar weight values are $W_1 = 114.8$ g/mol, $W_2 = 99.79$ g/mol, $W_3 = 84.755$ g/mol, and $W_{Ga} = 69.9$ g/mol. The density ρ and diffusivities D_n are dependent on the temperature at the point $\overrightarrow{x}_p$ on the substrate, with the density value found through equation (23) and the diffusivity values interpolated from literature values. The gas-phase flux is then used as the source term for gallium by the formula $S_1(t) = q^{M_G}(t)/W_{Ga}$ in the surface reaction layer which is described by the following modified ROSK model

$$\begin{aligned}
\dot{n}_1(t) &= \frac{q^{M_G}(t)}{W_{Ga}} - k_1 n_1(t) \\
\dot{n}_2(t) &= k_1 n_1(t) - k_{GaP}\left[S_p - n_3(t)\right] n_2(t) \\
\dot{n}_3(t) &= k_{GaP}\left[S_p - n_3(t)\right] n_2(t),
\end{aligned} \tag{27}$$

with n_1, n_2, and n_3 the moles per m^2 of Ga, activated Ga, and GaP, respectively. For this modified ROSK model we have chosen the rate constants to be $k_1 = 20$ s^{-1} (for transformation from gallium to activated gallium) and $k_{GaP} = 2000$ $m^2/(mol{\cdot}s)$ (for formation of gallium phosphide). Values of these parameters which better fit the physical surface processes should be found from experimental data as in Beeler et al. (1999), but our chosen values will serve for a proof-of-concept demonstration of the model and its control. The surface model has size $M_S = 3$ and can be written in vector form as $\dot{n}^{M_S} = f(n^{M_S}, q^{M_G})$.

Given a set of M_n basis functions $\{\Phi_{nk}\}$ for each species $n = 1, 2, 3$, we approximate the mass fraction of the nth species as a linear combination of the M_n basis elements

$$Y_n^{M_n}(t,\overrightarrow{x}) = \sum_{k=1}^{M_n} y_{nk}(t)\Phi_{nk}(\overrightarrow{x}). \tag{28}$$

Substitution of this approximation into a Galerkin approximation framework results in the following finite dimensional system for the species transport equation

$$\dot{y}^{M_G}(t) = A^{M_G} y^{M_G}(t) + B^{M_G} u(t), \tag{29}$$

where $M_G = \sum_{n=1}^{3} M_n$, A^{M_G} is an $M_G \times M_G$ matrix and B^{M_G} is an $M_G \times 1$ vector. The combined system, consisting of the gas phase model (29) linked to the modified ROSK model described by (27), is given by

$$\begin{bmatrix} \dot{y}^{M_G}(t) \\ \dot{n}^{M_S}(t) \end{bmatrix} = \begin{bmatrix} A^{M_G} y^{M_G}(t) \\ f\left(n^{M_S}(t), q^{M_G}(t)\right) \end{bmatrix} + \begin{bmatrix} B^{M_G} \\ 0 \end{bmatrix} u(t). \quad (30)$$

This can be written in terms of a single state vector as

$$\dot{x}^M(t) = \mathcal{A}(x^M(t))x^M(t) + \mathcal{B}u(t), \quad (31)$$

with $\mathcal{A}(x^M)$ an $M \times M$ matrix function of the combined state x^M, $\mathcal{B}$ a length M constant-valued vector, and u the single control input (the inlet TMG mass fraction). The initial state x_0^M is zero for all the gas-phase coefficients as well as all the surface species. We will track the gallium phosphide film thickness

$$\begin{aligned} d^M(t) &= V_{GaP} n_3(t) \\ &= H^M x^M(t), \end{aligned} \quad (32)$$

where $V_{GaP} = 12.2$ cm^3/mol is the molar volume of GaP and H^M is a constant output matrix.

To construct the tracking control problem for the combined system (31) and tracking signal (32) we consider the cost functional

$$J(x_0^M, u) = \frac{1}{2}\int_0^\infty \left[(d^M - d_T)^T Q_1 (d^M - d_T) + (\bar{d}^M)^T Q_2 \bar{d}^M + u^T R u\right] dt. \quad (33)$$

The weights are $R = 1$, $Q_1 = r_1$, and $Q_2 = r_2 I_M$, with I_M the $M \times M$ identity matrix and r_1 and r_2 two chosen design parameters. The desired film thickness trajectory $d_T(t)$ is a smoothed upward ramp function of growth from 0 to the final thickness of one monolayer of GaP, roughly 10^{-11} m.

The above tracking problem contains nonlinear dynamics in the surface reactions. In addition, we only have partial measurements as described above. Therefore, to implement a feedback control we must also include a state estimator/compensator. To this end, we implement the compensator based nonlinear feedback control, based on the solution to the SDRE as described in Section 2 and in Beeler et al. (2002). Since this is a tracking control problem, the feedback controller also includes a tracking variable, which is found using a two-point boundary value problem technique developed in Beeler et al. (2002). In the following simulation results, we use 5-terms power series in the expansion for the SDRE solution $\Pi(x)$. Fig. 4(a) depicts the resulting controlled film thickness tracking the growth of one monolayer of GaP (with dimensionless time units equivalent to 0.1 s). This figure depicts excellent tracking of the desired thickness profile, with the trajectory moving closer to the desired curve as the value of r_1 for the thickness weighting term in the cost functional increases, although even the $r_1 = 10^{-9}$ output is very close to the target profile. The control inputs u which were used to achieve these three controlled trajectories are plotted in Fig. 4(b), with the (scaled down) desired trajectory plotted there as well to show relative dynamics between the control action and target trajectory. The larger r_1 values (and so larger Q_1 and relatively smaller R in the cost functional) allow greater extremes in the control, which then force the thickness ramp to have sharper curves and more closely approach the rounded-ramp-shaped desired growth profile. The initial spike in the control input appears to be related to the slightly inaccurate initial estimated state which we used, although it may also be a very brief period in which the control/estimator needs to "learn" the behavior of the system.

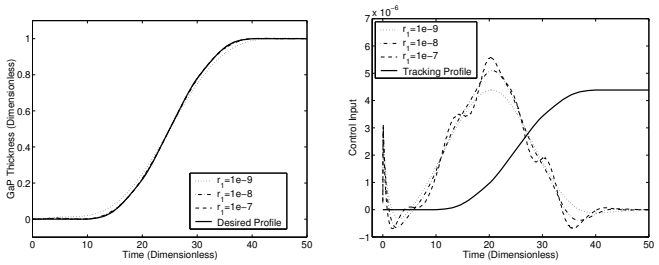

(a) (b)

Fig. 4. Each dimensionless time unit corresponds to 0.1 s. (a) Controlled growth film thickness profiles for various r_1 values. (b) Feedback control inputs for various r_1 values plotted against not-to-scale film thickness tracking profile

REFERENCES

Adams, B.M., Banks, H.T., Davidian, M., Kwon, H.D., Tran, H.T., Wynne, S.N., and Rosenberg, E.S. (2005). HIV dynamics: Modeling, data analysis, and optimal treatment protocols. *J. Comp. Appl. Math.*, 184, 10–49.

Banks, H.T., Beeler, S.C., Kepler, G.M., and Tran, H.T. (2002). Reduced order modeling and control of thin film growth in an HPCVD reactor. *SIAM J. Applied Mathematics*, 62(4), 1251–1280.

Banks, H.T., Kwon, H.D., Toivanen, J.A., and Tran, H.T. (2006). A state-dependent Riccati equation-based estimator approach for HIV feedback control. *Optim. Control Appl. Meth.*, 27, 93–121.

Banks, H., Lewis, B.M., and Tran, H.T. (2007). Nonlinear feedback controllers and compensators: A state-dependent Riccati equation approach. *Comput. Optim. Appl.*, 37, 177–218.

Barrett, J.W. and Elliot, C.M. (1986). Finite element approximation of the Dirichlet using the boundary penalty method. *Numer. Math.*, 49, 343–366.

Beeler, S.C., Tran, H.T., and Banks, H.T. (2002). State estimation and tracking control of nonlinear dynamical systems. *Int. Series Num. Math.*, 143, 1–24.

Beeler, S.C., Tran, H.T., and Dietz, N. (1999). Representation of GaP formation by a reduced order surface kinetics model using p-polarized reflectance measurements. *J. Appl. Phys.*, 86, 674–682.

Cloutier, J.R., D'Souza, C.N., and Mracek, C.P. (1996). Nonlinear regulation and nonlinear H_∞ control via the state-dependent Riccati equation technique: Part 1. Theory. In *Proceedings of the First International Conference on Nonlinear Problems in Aviation and Aerospace*. Daytona Beach, Florida.